environments

MDPI

Article

Optimization of Pyrolysis Parameters by Design of Experiment for the Production of Biochar from Sewage Sludge

Giacomo Cedrone [1], Maria Paola Bracciale [2], Lorenzo Cafiero [1], Michela Langone [3], Davide Mattioli [4], Marco Scarsella [2] and Riccardo Tuffi [1,*]

[1] Department for Sustainability, ENEA, Casaccia Research Center, Via Anguillarese 301, S. Maria di Galeria, 00123 Rome, Italy; giacomo.cedrone99@gmail.com (G.C.); lorenzo.cafiero@enea.it (L.C.)
[2] Department of Chemical Engineering, Sapienza University of Rome, Via Eudossiana 18, 00184 Rome, Italy; mariapaola.bracciale@uniroma1.it (M.P.B.); marco.scarsella@uniroma1.it (M.S.)
[3] Department for Sustainability, ENEA, Portici Research Center, P.le Enrico Fermi 1, 80055 Portici, Italy; michela.langone@enea.it
[4] Department for Sustainability, ENEA, Bologna Research Center, Via Martiri di Monte Sole 4, 40129 Bologna, Italy; davide.mattioli@enea.it
* Correspondence: riccardo.tuffi@enea.it; Tel.: +39-0630484335

Abstract: Sewage sludge management is a key concern in today's world. Improper disposal can lead to various environmental issues including air, water and soil pollution. Among the available technologies, thermal treatments, particularly pyrolysis, are gaining interest for their ability to reduce sewage sludge volume and to recover materials and energy from it. This study explored the influence of some relevant parameters in the thermal pyrolysis process. The design of experiment, named central composite design, was accounted to optimize temperature, heating rate and residence time in order to maximize the biochar yield and its CO_2 adsorption capacity. A two-factor interaction model provided a satisfactory interpretation of the results. Within the studied ranges, maximum values of 47.8 wt% and 0.514 mol CO_2/kg were obtained for the yield and CO_2 adsorption capacity, respectively. Two significant experiments were repeated in a different pyrolysis system highlighting how other factors (e.g., reactor geometry, granulometry, etc.) can influence the quantity and the quality of produced biochar. The biochar obtained under the best pyrolysis conditions was characterized by a surface area of 124 m^2/g and an ash content of 61 wt%. Lastly, the theoretical energy balance showed that the drying process is the main energy-intensive step in the pyrolysis of sewage sludge.

Keywords: sewage sludge; pyrolysis; biochar; design of experiment; carbon dioxide adsorption; yield

Citation: Cedrone, G.; Bracciale, M.P.; Cafiero, L.; Langone, M.; Mattioli, D.; Scarsella, M.; Tuffi, R. Optimization of Pyrolysis Parameters by Design of Experiment for the Production of Biochar from Sewage Sludge. *Environments* **2024**, *11*, 210. https://doi.org/10.3390/environments11100210

Academic Editor: Sergio Ulgiati

Received: 21 August 2024
Revised: 16 September 2024
Accepted: 19 September 2024
Published: 24 September 2024

1. Introduction

The management of sewage sludge continues to pose significant challenges, due to the large volumes produced, environmental impacts and associated costs [1]. Recognizing the value of sludge rich in organic substances and nutrients, the regulatory framework for sludge management encourages a shift towards sustainable and circular practices. National policy frameworks are evolving in response to several initiatives, including the Circular Economy Action Plan [2], the Bioeconomy Strategy [3], the new Fertilizing Products Regulation [4], the Farm to Fork Strategy [5], the EU Biodiversity Strategy [6], the EU Soil Strategy [7] and the EU Climate Action [8].

Currently, Italy is the third largest producer of municipal sludge in Europe after Germany and Spain, with 3.2 million tons per year, approximately 10 wt% of European production [9]. At the national level, 52 wt% of sewage sludge is disposed of through landfill or incineration, while 46 wt% is recovered, primarily for agricultural use or soil restoration [10]. The recovery of inorganic substances is minimal, and energy recovery in sludge treatment hubs, through methods like anaerobic digestion, pyrolysis, or co-incineration is very low, only 1 wt%. Considering that the resolution of the infringement

procedures is expected to result in an additional 800,000 tons of sewage sludge [11] and that regulations on agricultural recovery are becoming more restrictive, current sewage sludge management practices in Italy are likely to encounter substantial challenges.

Sewage sludge management should include a diversified territorial approach that considers the specificity of the sludge and the territory, the principles of the waste hierarchy and the circular economy, enhancing the system's flexibility. It is beneficial to focus on the overall system and to develop sewage sludge treatment hubs that apply different criteria and technologies as appropriate, including innovative solutions. Thermal treatments are gaining importance because of their ability to reduce the volume of sludge to be managed and to recover materials and energy. Among these treatments, pyrolysis stands out as an effective solution for sewage sludge processing, producing valuable products such as biochar, bio-oil and gas that can be utilized as fuels or feedstocks [12].

Simultaneously, numerous studies are underway to reduce CO_2 emissions into the atmosphere, exploring alternatives to lower CO_2 levels and considering methods to control the release of this greenhouse gas from industrial activities. The three primary gas capture and sequestration methods involve the use of liquid absorbents, solid adsorbents and membranes [13]. Among them, adsorption technologies have garnered significant attention due to their low deployment cost, high selectivity and recovery for CO_2 and environmental friendliness [14]. Recent innovations have led to the investigation of various sorbents including activated carbons, graphene-based materials, amine salt polymer composites/amine polymers, silicas and silica-amine composites, zeolites and metal oxide-based sorbents and metal–organic frameworks [15]. Recent progress has proposed the biochar from pyrolysis of sewage sludge as low-cost sorbents for carbon capture and sequestration through adsorption [16].

The porous nature of biochar produced by pyrolysis from different biomasses creates a high surface area (up to 500 m^2/g) [17] that together with its surface functional groups and carbon-rich composition contributes to its effectiveness in carbon capture, through both physical and chemical sorption [16,18–20]. However, the potential applications of a sewage sludge biochar as an effective adsorbent highly depends on its morphological structure and physicochemical properties, which in turn depend on the characteristics of the feedstock and the conditions of the pyrolysis process [19,21,22]. Nevertheless, conducting experiments across the entire domain of pyrolysis process parameters and examining the impact of simultaneous changes in multiple factors would require numerous trials, which are both expensive and time-consuming. Thus, the importance of the statistical method called design of experiments (DoE) has been widely recognized in optimizing synthesis processes, due to its systematic approach to experimentation, improving product quality, increasing efficiency and reducing costs by enabling precise control and analysis of multiple variables simultaneously. Recently, DoE was applied to study the synthesis of CO_2 adsorbent materials and pyrolysis processes [23,24].

This study explored the potential of using the biochar produced by the pyrolysis of sewage sludge as a valuable material for the adsorption of CO_2. More in detail, this work adopts a DoE approach to develop an understanding of the effects of pyrolysis design factors, namely, pyrolysis temperature, heating rate and residence time on biochar yield and CO_2 adsorption capacity. Furthermore, two sets of representative experiments from DoE were repeated in a different and more realistic pyrolysis system and the produced biochars underwent a chemical-physical characterization. Lastly, a theoretical energy balance was calculated for the drying and pyrolysis phases of a centrifuged sewage sludge outgoing a wastewater treatment plant. Figure 1 shows the scheme of the phases of this study.

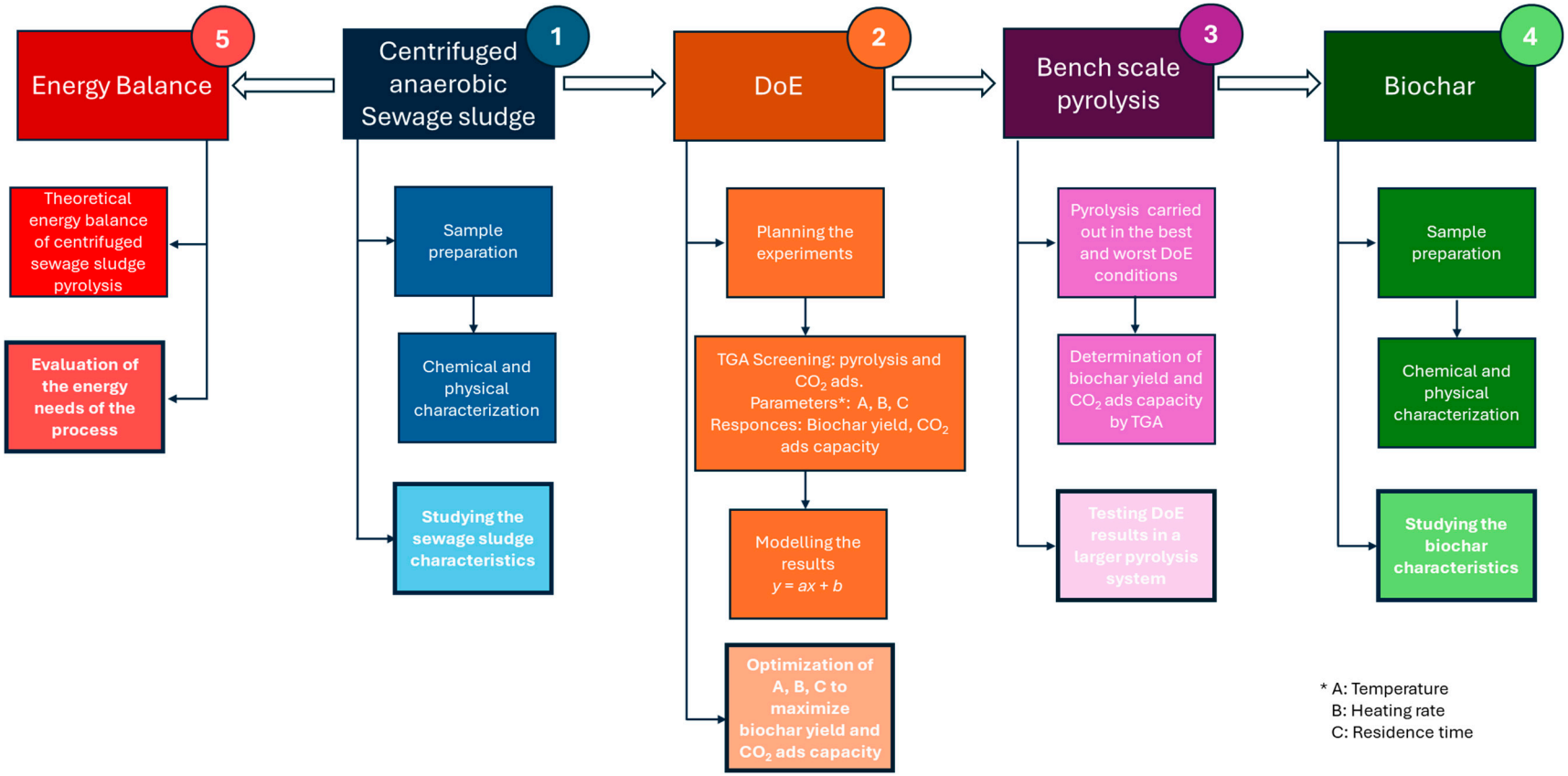

Figure 1. Scheme reporting the investigation phases of this study.

2. Materials and Methods

2.1. Sample Characterization

The municipal sewage sludge was supplied by a civil wastewater treatment plant located in Central Italy. The sample (5 kg) was an anaerobically digested sewage sludge, centrifuged to a final water content of 75.6 wt%.

The sewage sludge was dried in an oven at 105 °C for 24 h to remove the moisture and to stop further biodegradation processes. Subsequently, 500 g of dried sewage sludge was ground up to particles smaller than 0.5 mm using a Retsch SM 2000 cutting mill, equipped with a 0.5 mm sieve, and homogenized. This sample underwent chemical and thermal characterization, as well as was used in the DoE pyrolysis tests.

Proximate analysis was performed to determine moisture, ashes, volatile matter and fixed carbon content by using a thermogravimetric analyzer (Mettler Toledo TG/DSC1, Columbus, OH, USA) and adopting the temperature program reported in Table S1. Dried sewage sludge samples of 30–40 mg were weighed to the nearest 0.001 mg in a 150 µL alumina pan for proximate analysis.

Ultimate analysis was carried out to determine the elemental composition of the sample adopting a Macro VARIO Cube elemental analyzer (Langenselbold, Germany). Carbon (C), Hydrogen (H), Nitrogen (N) and Sulphur (S) were directly measured, while Oxygen (O) was calculated as the difference in all determined elements and the ash content to 100 wt%. The samples for the ultimate analysis were prepared in tin boats weighing 20–30 mg to the nearest 0.01 mg of dried sewage sludge with the same amount of the oxidizing agent, tungsten trioxide.

Thermal analysis was carried out using the Mettler Toledo TG/DSC1 and a differential scanning calorimeter (DSC), model 250 from TA Instruments (Milford, MA, USA). For TG analysis (TGA), a 10.0 ± 0.1 mg sample was weighed in a 70 µL alumina pan and heated from 25 °C to 900 °C at 10 °C/min in a nitrogen flow (60 mL/min). A preliminary 'blank experiment' was performed to correct the TG baseline accounting for the gas buoyancy effect over the whole investigated temperature range. For DSC analysis, approximately 10.0 ± 0.1 mg of sample were loaded into Tzero aluminum pans and heated up from 50 to 600 °C at a rate of 10 °C/min under a nitrogen atmosphere (50 mL/min). The results of the thermal analysis were used to set the pyrolysis experiments and to calculate the theoretical energy balance.

The high heating value (HHV) was measured using a Mahler bomb calorimeter IKA C5000 (Staufen, Germany). The sample (0.5 g weighed to the nearest 0.001 g) was weighed in a polyethylene bag with a known HHV and placed into the bomb. A buffer solution of 10 mL $NaHCO_3/Na_2CO_3$ was added to the bomb to capture the acid gasses evolved during the combustion of the sewage sludge. This solution was quantitatively recovered, diluted with milli-Q water in a 100 mL volumetric flask and analyzed by ionic chromatography (883 Basic IC plus Metrohm Ion Chromatography, Herisau, Switzerland) for the content of Cl and Br.

Finally, the low heating value (LHV) was calculated with the following equation:

$$LHV = HHV - 2.5\,(9\,(HyC) + (HuC)) \quad (1)$$

where HyC is the hydrogen content, and HuC is the moisture content of the sample expressed as fractions.

Each measurement was replicated three to five times.

2.2. Pyrolysis and CO_2 Adsorption Experiments through TGA

In this study, the optimum operating conditions for biochar production were studied in terms of yield and adsorption capacity using DoE software (Design Expert ver. 13, Stat-Ease, Minneapolis, MN, USA). The effect of three variables (pyrolysis temperature, heating rate and residence time) on biochar yield (expressed as wt% with respect to the initial mass of the sewage sludge) and its CO_2 adsorption capacity (expressed as moles of adsorbed CO_2

per kilogram of biochar) was examined. These three parameters are recognized as essential in the pyrolysis studies [25]. Considering that the operating parameters studied could also interact with each other and that these factors have already been identified as influencing the process, a "response surface design" was used, more precisely a Central Composite Design (CCD). This type of DoE requires performing a number (N) of experiments (runs) equal to

$$N = 2^f + 2f + 1 \quad (2)$$

where f is the number of parameters studied. These experiments were carried out by varying the parameters within a symmetric domain, consisting of a cubic space, (Figure 2) where the vertices of the domain (factorial points) are represented by coordinates +1 and −1, the axial points (sometimes called "star" points) are represented by the coordinates 0, α, α and the central point by coordinates 0, 0, 0.

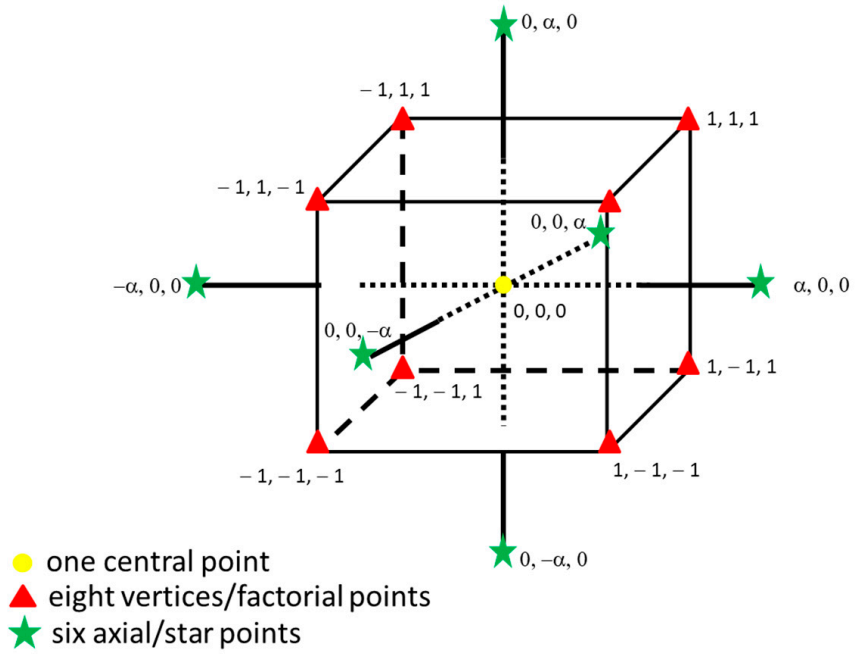

Figure 2. Representation of the central composite full factorial DOE with the fifteen experiments.

The experiment corresponding to the central point of the domain (0, 0, 0) was repeated six times to evaluate the experimental error. Then, N was twenty. From the literature [25–27] and from the thermal behavior of the sample, the operating ranges of the pyrolysis were set and the values corresponding to the CCD factors are reported in Table 1. The use of medium/high temperatures is also recommended to exploit gas and bio-oil produced during the pyrolysis of sewage sludge. Table 2 reports the details of all runs.

Table 1. Experimental parameters (temperature, heating rate and residence time) of the set of pyrolysis for the production of biochar and relative coded variables of the DoE CCD.

Factor	Parameter	Unit of Measure *	$-\alpha$	$+\alpha$	−1	+1	0
A	Temperature	°C	450.00	650.00	490.54	609.46	550.00
B	Heating rate	°C/min	5.00	50.00	14.12	40.88	27.50
C	Residence time	min	30.00	180.00	60.41	149.60	105.00

* For the TGA the experimental parameters were rounded to the nearest 0.5 unit.

Table 2. Experimental parameters (Factor A: Temperature/°C. Factor B: Heating rate/°C/min. Factor C: Residence time/min) of the biochar production following the DoE CCD.

Run	Factor A (°C) *	Factor B (°C/min) *	Factor C (min) *
1	550.00	27.50	105.00
2	490.54	14.12	149.60
3	490.54	40.88	60.41
4	450.00	27.50	105.00
5	550.00	50.00	105.00
6	550.00	27.50	30.00
7	550.00	27.50	180.00
8	490.54	14.12	60.41
9	550.00	27.50	105.00
10	490.54	40.88	149.60
11	550.00	5.00	105.00
12	650.00	27.50	105.00
13	550.00	27.50	105.00
14	609.46	14.12	60.41
15	550.00	27.50	105.00
16	609.46	14.12	149.60
17	609.46	40.88	149.60
18	550.00	27.50	105.00
19	550.00	27.50	105.00
20	609.46	40.88	60.41

* For the TGA the experimental parameters were rounded to the nearest 0.5 unit.

Pyrolysis experiments and CO_2 adsorption capacity measurements were carried out in two consecutive steps using the Mettler Toledo TG/DSC1. TGA was chosen as a pyrolysis reactor for its high precision and accuracy in temperature and heating rate control, the use of small amounts of sample, ease in the experiment preparation and the possibility of carrying out the pyrolysis and the adsorption experiments in sequence. For the TGA the experimental parameters were rounded to the nearest 0.5 unit. A sample of 80 ± 1 mg of dried sewage sludge was placed into a 150 µL alumina pan and underwent pyrolysis at the operating conditions set by DoE software. Nitrogen flow rate (100 mL/min) and size particles of sewage sludge (<0.5 mm) were kept constant among the different experiments.

The yield of biochar was calculated as the residual mass with respect to the initial mass of the sample. Once the pyrolysis was completed, the biochar was cooled to 25 °C with a cooling rate of 10 °C/min and N_2 at 100 mL/min. After the pyrolysis step, the biochar CO_2 adsorption capacity was measured in isothermal conditions: the sample was kept at 25 °C for 5 min under N_2 (flow, 20 mL/min); the CO_2 adsorption started opening the valve and flowing CO_2 with 155 mL/min flow rate for 45 min. The CO_2 adsorption capacity was calculated according to the positive mass change in the sample during the isothermal adsorption. Table 3 summarizes the steps of the experiments.

Table 3. TGA thermal program for each run i of DoE experiments.

Step	Sample	Atmosphere	Temperature Program				
			T_i (°C)		T_f (°C)	β = dT/dt (°C·min^{-1})	Δt Isotherm (min)
Pyrolysis	Dried sewage sludge	N_2 at 100 mL/min	25	$T_{run\ i}$	$T_{run\ i}$	$\beta_{run\ i}$	-
			$T_{run\ i}$		25	-	$\Delta t_{run\ i}$
						10	-
CO_2 ads	Biochar	N_2 at 20 mL/min	25			-	5
		CO_2 at 155 mL/min	25			-	45

T_i and T_f, initial and final temperature, respectively. β, heating rate. Δt, residence time. Run i, i-th run of the DoE CCD. Hyphen indicates that the variable is not applicable.

Finally, the results of all experiments were processed by Design Expert ver. 13 software for statistical analysis and the final equations of the biochar yield and its adsorption capacity as a function of the three independent variables, temperature, heating rate and residence time were extracted. The significance level was set at 0.05.

2.3. Pyrolysis through a Bench Scale Semi-Batch Reactor

In order to verify the results of DoE in a different pyrolysis system as well as to produce an amount of biochar sufficient for its characterization, two significant experiments were repeated in a larger pyrolysis reactor. The "best experiment" corresponds to the DoE run (in terms of temperature, heating rate and residence time) that produced a combination of the highest yield and CO_2 adsorption capacity biochar, while the "worst experiment" corresponds to the DoE run that produced the lowest yield and CO_2 adsorption capacity biochar. A bench scale semi-batch reactor was used for the pyrolysis process: the dried sample was loaded before the experiment, whereas the vapors/gasses that evolved during the sewage sludge degradation, were progressively removed as they were formed, thanks to the action of the carrier gas. The reactor is a steel tube of 70 mm internal diameter with a boat for the sample, placed in its middle zone. The reactor was inserted in an electrical furnace (model LTF 12/75/610 Lenton, equipped with a control system specifically designed and made by Innomec S.r.l., Roma, Italy). Temperature control was performed inside the reactor using a temperature probe. Samples of 20 g of dried sewage sludge, as it was (Figure S1), were loaded in the boat of the reactor. The whole set-up was washed for 5 min with 25 L/min of N_2 for the atmosphere inertization. N_2 generator (Mistral Evolution LCMS, VICI DBS, Houston, TX, USA) was used to produce N_2 with a purity of 98 v/v%.

The temperature program to replicate the "best experiment" of the DoE CCD consisted of the following steps: heating from 25 to 491 °C at 20 °C/min, maintaining 491 °C for 150 min and cooling to 25 °C. Instead, for the "worst experiment" resulting from the DoE CCD the temperature program was heating from 25 to 610 °C at 20 °C/min, maintaining 610 °C for 150 min and cooling to 25 °C. It is important to note that the heating rate of the electrical furnace is about 20 °C/min and it cannot be modified. Thus, "best" and "worst" experiments were chosen among the four runs that had the closest heating rate to that of the furnace, i.e., 14.1 °C/min. All the steps of both programs were carried out in a nitrogen atmosphere at a flow rate of 1.2 L/min. This value of N_2 flow rate was chosen to keep the velocity of the gas in the reactor and in the TG equal to about 0.53 m/s. The biochar produced was collected and weighed to calculate the yield of the pyrolysis process. It was then labeled as "best" or "worst" biochar depending on the experiment used. The vapor and gas fractions were not collected nor analyzed.

The two biochars were <0.5 mm milled and subjected to CO_2 adsorption experiments in the TG/DSC1. A sample of 20.0 ± 0.1 mg of biochar was placed in a 150 µL alumina pan and underwent the following temperature program: heating from 25 °C to the biochar synthesis temperature minus 10 °C with a heating rate of 20 °C/min under N_2 (flow 20 mL/min), cooling to 25 °C at 10 °C/min under N_2 (flow 20 mL/min), maintaining 25 °C for 5 min under N_2 (flow 20 mL/min), maintaining 25 °C for 45 min under CO_2 (flow 155 mL/min). The first two steps were necessary to strongly clean the biochar without causing further thermal degradation of the material. The second two steps regarding CO_2 adsorption were carried out in the same conditions as the DoE CCD experiments.

The "best" and "worst" biochar underwent proximate and ultimate analysis and LHV determination, as described in Section 2.1. The biochar sample's surface areas were also determined using the N_2 adsorption technique. N_2 adsorption–desorption isotherms were collected using volumetric equipment (Micromeritics 3Flex analyzer, Norcross, GA, USA) at temperatures of −196 °C, over a relative pressure (p/p^0) range from 0.01 to 0.99. Before the analysis, the samples were outgassed at 250 °C under N_2 flow for 24 h. The specific surface area (SSA), pore volume and average pore diameter were determined using the BET and BJH equations, respectively. The T-plot' statistical thickness method was used to calculate micropore volume and micropore surface area.

3. Results and Discussion

3.1. Sewage Sludge Characterization

The results of the proximate analysis are shown in Table 3. The sample still had a moisture content due to incomplete dehydration or to adsorption of moisture from the air, as it had not been stored in a dry environment. The sample presented an interesting content of volatile matter, and a lower amount of fixed carbon compared to other materials that can be used for char production, such as lignocellulosic biomass or some plastics [28,29]. Then, char production cannot be separated from the valorization of the gaseous and liquid products in a pyrolysis process of sewage sludge. It is important to note that the sample was characterized by a high ash content (around 30 wt%), which means a high content of inorganic elements accumulates in the produced biochar. Iron, calcium, potassium and magnesium are usually the main inorganic elements, but the presence of heavy metals cannot be excluded a priori [30]. The values of proximate analysis were in the wide range reported in the literature [28].

Table 4 also shows the elemental composition of the sample. C and H accounted for about 41 wt% while the heteroatoms (N, S, O, Cl) accounted for almost 30 wt%. Elemental analysis also agreed with values found by other researchers [28]. Sewage sludge in comparison to lignocellulosic biomass had higher N and S concentrations (S content is comparable to that of coal). Dead microorganisms are the main source of N and S in sewage sludge. High concentrations of heteroatoms decrease the quality of pyrolysis products that, in the case of bio-oil, will have to undergo an upgrading process before being used as fuel [31]. The presence of O reduces the LHV, while high N and S contents would lead to the formation of NO_x and SO_x during combustion with consequent environmental problems [32]. On the contrary, the halogen concentration can be considered not relevant.

Table 4. Proximate, ultimate and LHV analysis of the dried sewage sludge.

	Moisture (wt%)	**Volatile Matter (wt%)**	**Fixed Carbon (wt%)**	**Ashes (wt%)**	**C (wt%)**	**H (wt%)**	**N (wt%)**	**S (wt%)**	**O * (wt%)**	**Cl (wt%)**	**Br (wt%)**	**HHV (MJ/kg)**
Sewage sludge	2.4 ± 0.6	57.8 ± 0.3	10.7 ± 0.1	29.2 ± 0.3	36 ± 1	5.3 ± 0.2	5.8 ± 0.2	1.1 ± 0.1	22.2	0.050 ± 0.002	n.d.	15.0 ± 0.3

* Oxygen is calculated by difference. n.d.: not detected.

Figure 3a shows the thermal behavior of the sample through TG and derivative TG (DTG) curves, highlighting the temperatures and mass variations during the thermal degradation under an inert atmosphere. Except for the first mass loss (below 170 °C) due to water evaporation, the pyrolysis of the sample occurred in four steps. The first three, in the range 170–590 °C with a mass variation of about 40 wt%, correspond to the main decomposition phase in sewage sludge, involving the emission of organic volatile substances [33]. The DTG curve in this temperature range shows two overlapping peaks with maxima around 280 °C and 320 °C, along with a shoulder near 420 °C, attributed to the decomposition of carbohydrates and proteins and aliphatic compounds, respectively. The fourth isolated step occurring at around 700 °C with a slight mass loss of 3 wt%, is mainly attributed to the decomposition of inorganic materials, such as calcium carbonate [33]. At the end of the analysis, the TGA curve was characterized by weight loss with an approximately constant rate, not reaching a plateau. The final residue (39 wt%) appeared as ash covered by a layer of coke.

As shown in Figure 3b, the DSC curve exhibits four main transformations. The extremely large endothermic peak before 200 °C was attributed to the latent heat of water vaporization resulting from the moisture content and the decomposition of the bonded hydrated compounds in the sample. The subsequent endothermic peaks, occurring between approximately 200 and 380 °C, corresponded to the major peaks in the DTG curve, indicating that these reactions were accompanied by intensive mass loss.

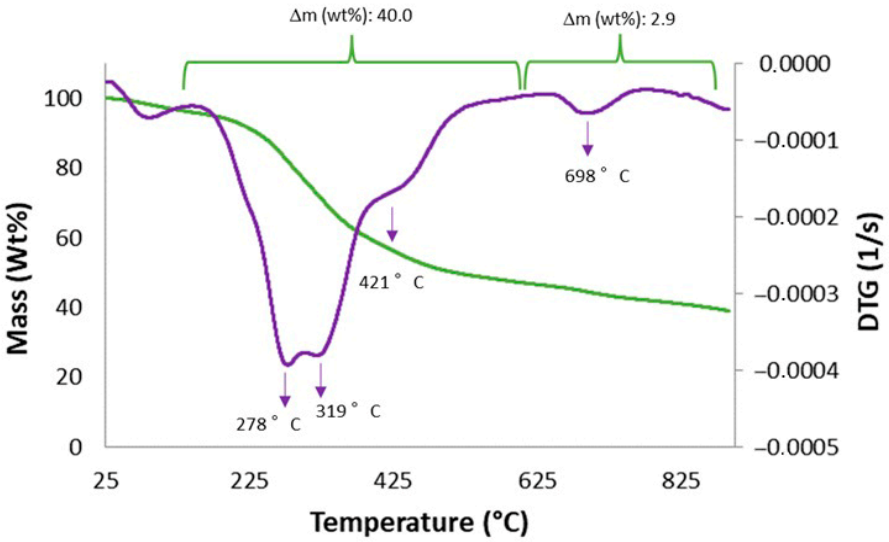

(**a**)

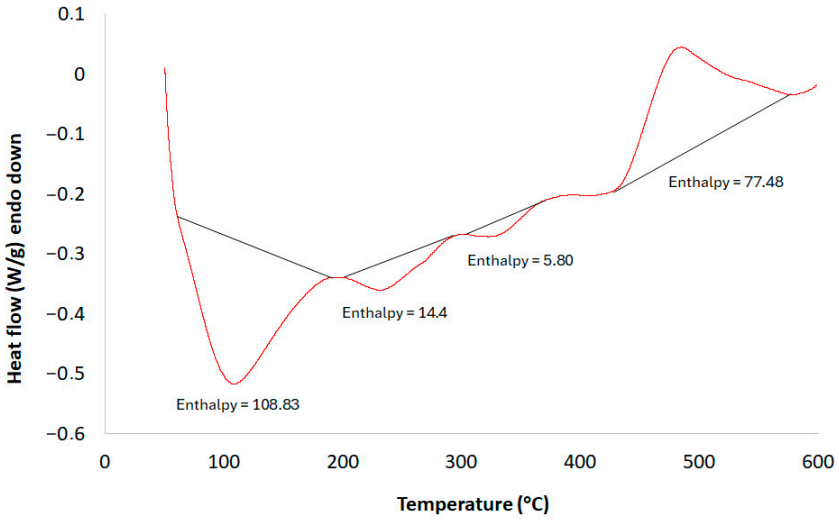

(**b**)

Figure 3. TG (green) /DTG (purple) (**a**) and DSC (red) (**b**) curves of the sewage sludge at 10 °C/min under an inert atmosphere.

As the temperature increased further, an exothermic reaction occurred between 460 and 560 °C due to the charring process, which involved the interaction between organic matter and the volatile compounds released during the earlier stages of decomposition, and the transformation of inorganic materials into carbonates [34,35].

The total energy required for the endothermic reactions was 129 J/g, while the exothermic one amounted to 78 J/g.

To conclude the sample characterization, an HHV of 15.0 MJ/Kg was determined by bomb calorimetry, in line with other values found in the literature for sewage sludge from wastewater treatment [36]. Low HHV values of dried sewage sludge lie in the fact that the sample has a high content of non-combustible elements, such as inorganic ones and O. Taking into account the measured values of H and moisture, the LHV was calculated using Equation (1) and resulted in 13.75 MJ/kg.

3.2. Optimization of Design Parameters for Biochar Production

Table 5 reports the results obtained from pyrolysis runs in terms of biochar yields and its CO_2 adsorption capacity.

Table 5. Yield and CO_2 adsorption capacity of the biochars produced by different pyrolysis conditions.

Run	Yield (wt%)	Adsorption Capacity (mol CO_2 ads/kg)
1	44.76	0.468
2	46.23	0.491
3	46.00	0.484
4	47.80	0.454
5	43.10	0.428
6	46.00	0.445
7	43.85	0.397
8	46.10	0.458
9	44.00	0.417
10	46.15	0.390
11	46.20	0.461
12	40.90	0.397
13	44.60	0.450
14	44.70	0.433
15	44.50	0.459
16	42.60	0.514
17	38.20	0.316
18	44.00	0.441
19	44.40	0.421
20	43.14	0.457

The runs carried out gave results in terms of CO_2 adsorption in the range of 0.316–0.514 mol CO_2/kg, where run 16 (609.5 °C, 14.1 °C/min and 149.6 min) recorded the best result. Literature reports that biochar obtained from pyrolysis of sewage sludges shows values of adsorption capacity around 0.4–0.6 mol CO_2/kg [37,38], in line with the values obtained by this study. Biochar produced from different types of biomasses and with different procedures has adsorption capacities between 0.4 and 2.8 mol CO_2/kg [38]. The reported ranges are broad, and it should be taken into consideration that it is difficult to compare the adsorption capacities of biochar obtained from similar feedstock as well as from similar pyrolysis conditions because the different experimental parameters, such as adsorption temperature, CO_2 pressure, granulometry or the apparatus used to carry out the analysis, greatly influence the result. Other solid materials such as zeolites produced from waste materials reach values between 0.1 and 5.1 mol CO_2/kg [23].

Among best-performing methodologies, absorption in aqueous solutions (e.g., aqueous solutions of alkanolamines) is one of the most industrially used, even if expensive management of the saturated solutions is required [39]. To be competitive with current carbon capture methodologies, a new solid material should capture 3–4 mol CO_2/kg [39]. In the case of sorbents from waste, the circular approach with the use of low-cost materials instead of virgin raw resources and the saving on waste disposal should also be taken into account. Furthermore, biochar is only one of the products of the pyrolysis of sewage sludge and an overall feasibility study of the process will also have to take into consideration the exploitation of bio-oil and gas. Biochar could also undergo an activation process through a chemical or physical agent to improve its adsorption capacity.

Regarding the biochar yield, values vary between 38.2 and 47.8 wt%, where test 4 (450 °C, 27.5 °C/min and 105 min) obtained the best result. The yields align with those reported in the literature, where authors observed values in the range of 25–64 wt% [40,41]. Also, in this case, the high variability depends on the different feedstocks and operating conditions. Because of the high ash content (29.2 wt%) in the sewage sludge and ash accumulating into the pyrolysis solid residue, the yields of the real carbonaceous substance

drop to 9–18.6 wt%. Thus, biochar is mainly composed of ashes with values between 76 and 61 wt%. Table 6 shows the statistical data necessary for evaluating the goodness of the models for the adsorption capacity and yield.

Table 6. Statistical parameters for the evaluation of the two models.

Optimized Results	Model	*p*-Value	Lack of Fit *p*-Value	Adj-R^2	Pred-R^2
CO_2 adsorption capacity	2FI	<0.0001	0.4268	0.7396	0.5892
Yield	2FI	<0.0001	0.1147	0.9506	0.8369

2FI: two-factor interaction model. *p*-value: significance value, probability of observing a value of the ratio between the variance of the experimental data and the variance of the residuals greater than that calculated on the experimental data, assuming that the null hypothesis is true. lack of fit *p*-value: comparison of the value of the residuals obtained from the model with the experimental error obtained from the replica of the test at the central point of the domain. Residuals significantly greater than the experimental error highlight a model that is not suitable for "fitting" the experimental data. Adj-R^2: proportion of the variation in the dependent variable that is predictable from the independent variable(s). It is a modified version of R^2 that has been adjusted for the number of predictors in the model. Pred-R^2: indication of how well the model predicts responses for new observations. The difference between Pred-R^2 and Adj-R^2 should be <0.2.

Regarding the CO_2 adsorption capacity of biochar, Design Expert selected a two-factor interaction model (2FI). The model was significant since the *p*-value was less than 0.05. The lack of fit is not significant (>0.05): a non-significant lack of fit indicates a good ability of the model to "fit" the obtained data. The values of Adj-R^2 and Pred-R^2 are in satisfactory agreement (their difference is less than 0.2), even if their values are only medium-high. This means that the model is able to interpret the variance of the obtained data, but higher values would have guaranteed greater reliability.

The following equations describe the correlation between the adsorption capacity and the studied parameters in terms of coded and actual factors.

$$CO_2\ ads = 0.439 - 0.0146 \times \mathrm{A} - 0.0224 \times \mathrm{B} - 0.0148 \times \mathrm{C} - 0.0436 \times \mathrm{BC} \quad (3)$$

$$CO_2\ ads\ (\mathrm{mol/kg}) = 0.443292 - 0.000245 \times \mathrm{A} + 0.006006 \times \mathrm{B} + 0.00168 \times \mathrm{C} - 0.000073 \times \mathrm{BC} \quad (4)$$

where A, B and C are the DoE CCD factors, corresponding to temperature, heating rate and residence time, respectively.

The coded Equation (3) "weights" each factor and their interactions for the CO_2 adsorption, while the actual Equation (4) can be used to make predictions about the response of the biochar in different synthesis conditions. From Equation (3) it can be observed that all the analyzed factors individually influence the adsorption of CO_2, although the heating rate (B) is the parameter that weighs the most. However, the two-factor interaction term between the heating rate and the residence time (BC) has the highest "weight" (coefficient 0.0436). On the contrary, the other two-factor interactions (AC and AB) for the CO_2 adsorption capacity of biochar are not significant with the model obtained from these results. Equation (4) revealed that the model predicts the experimental values of CO_2 adsorption capacity quite well. The mean relative error between the experimental and calculated values was 4%, corresponding to an absolute error of $\pm$0.02 mol/kg on the values of CO_2 adsorption capacity. Figure S2 summarizes this issue, plotting actual versus predicted values. Figure S3 shows the statistical distribution of the residuals of the different runs, defined as the difference between values predicted by the model and the actual ones. The points followed the red line, highlighting a good normal distribution. Figure S4 represents how the predicted values by the model influenced the residuals: no trends were observed in the plot and the so-called "megaphone effect" (high and low residuals correspond to high and low predicted values respectively, taking the shape of a megaphone) was absent. Figure S5 shows the trend in the residuals as a function of the runs: the distribution of the residuals is random as it should be, corresponding to a lack of trends or the presence of variables not considered within the process. The two red lines above and below in the last two figures identify the outliers (the values beyond red lines) among the different

runs, i.e., anomalous and aberrant values that are clearly far from the others in a set of results. As can be observed from Figures S3 and S4, there are no outliers among the values of adsorption capacity.

Figure 4 shows the trend of CO_2 adsorption capacity as a function of the biochar synthesis parameters: heating rate and residence time at two different temperatures (490.5 and 609.5 °C). Comparing Figure 3a,b, it can be noted that the shape of the two 3D curves is very similar, they are quite simply translated and, consequently, heating rate and residence time did not change their way to influence the CO_2 adsorption capacity as the temperature changed. Generally speaking, in the investigated temperature range, the CO_2 adsorption capacity increased (from 450 to 500 °C) and then decreased (from 500 to 650 °C) with increasing temperature, although the best result was found at 609.5 °C (14.12 °C/min and 49.6 min, run 16). Lu and collaborators [42] found that the surface area of biochar increased with temperature, but it was reduced for biochars obtained at 550–650 °C, possibly owing to the pore enlargement phenomenon because of a loss of volatiles in the intermediate thermoplastic phase. The formation of a macro-porous structure decreases the specific surface area, and consequently, the CO_2 adsorption capacity. These effects can be explained considering that higher temperatures favored the volatilization of solid matter with the consequent lower formation of biochar per unit mass of solid residue. Furthermore, higher CO_2 adsorption capacity was obtained for slow heating rates at long residence times and for short residence times at high heating rates. Also, the influence of heating rate and residence time on the CO_2 adsorption capacity was related to the release of volatile matter during pyrolysis. As an example, a slow heating rate and long residence time gave the time for the development of a porous structure during the thermal degradation of sewage sludge. On the contrary, long residence time with a fast heating rate caused an excessive production of volatile matter with the consequent formation of a macro-porous structure.

Regarding biochar yield, a 2FI model was used for the analysis of the results. We found out (Table 6) that the model is significant (p-value < 0.05), while the lack of adaptation is not significant (lack of fit > 0.05). Furthermore, the Adj-R^2 and Pred-R^2 are high and close together. These statistical parameters identified an accurate model for the prediction of biochar yields of a pyrolysis process. Equations (5) and (6) express the correlation between the biochar yield and the three investigated factors in terms of coded and actual factors, respectively:

$$\text{Yield} = 44.36 - 2.01 \times A - 0.8313 \times B - 0.7598 \times C - 0.7225 \times AB - 0.9150 \times AC - 0.3525 \times BC \quad (5)$$

$$\text{Yield (wt\%)} = 31.0766 + 0.027412 \times A + 0.499428 \times B + 0.188999 \times C - 0.000908 \times AB - 0.000345 \times AC - 0.000591 \times BC \quad (6)$$

where A, B and C are the DoE CCD factors, corresponding to temperature, heating rate and residence time, respectively.

Unlike CO_2 adsorption capacity, all factors and all their binary interactions were found to be significant for the biochar yield. Temperature is the factor with the highest weight (coefficient equal to 2.01), as was foreseeable for the product yields of a pyrolysis process since it controls the cracking reactions of the organic matter [43].

In Figures S6 and S7, the points are quite well distributed along the lines, showing a good normal distribution of the results. The mean relative error between the experimental and calculated values was around 0.7%, corresponding to an absolute error of ±0.3 wt% on biochar yields. From Figures S8 and S9, it is evident that there was not a "megaphone effect" and the distribution of the residuals had no trend. However, run 2 was recognized as a possible outlier, lying on the low red borders of the two Figures.

Figure 5 shows the trends in biochar yield as a function of the heating rate (B) and residence time (C) at 490.5 and 609.5 °C, as an example. Biochar yield achieves its optimum between 300 and 500 °C and, once the temperature of complete carbonization is reached, biochar yield is reported to constantly decrease with temperature [40,44].

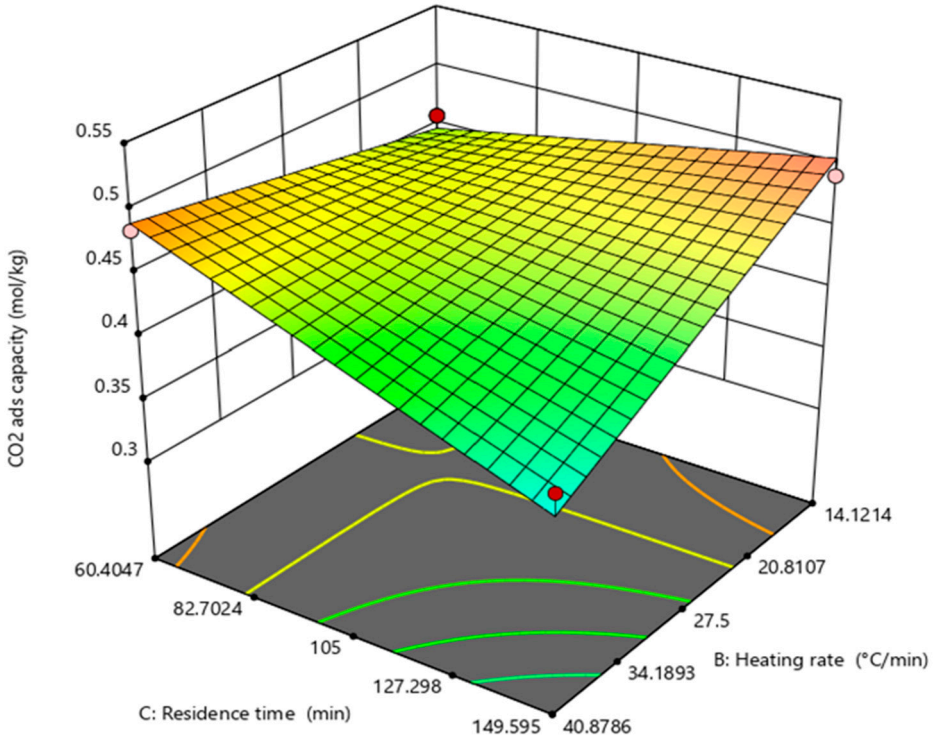

(**a**)

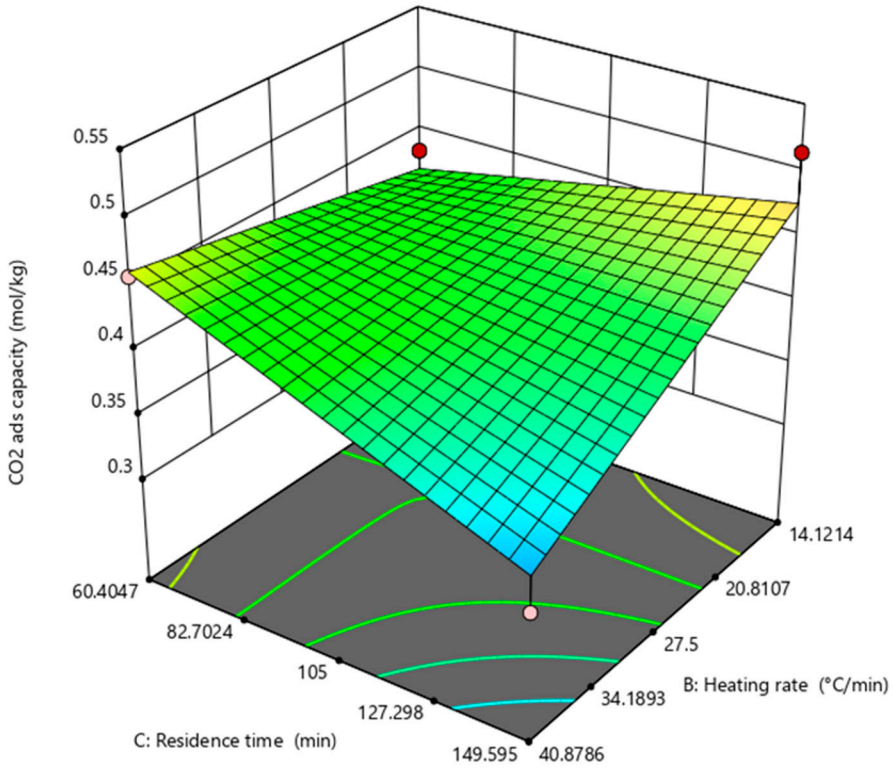

(**b**)

Figure 4. Response of CO_2 adsorption capacity ($molCO_2/kg$) to residence time and heating rate at 490.5 °C (**a**) and 609.5 °C (**b**). Red and pink dots indicate the domain limits.

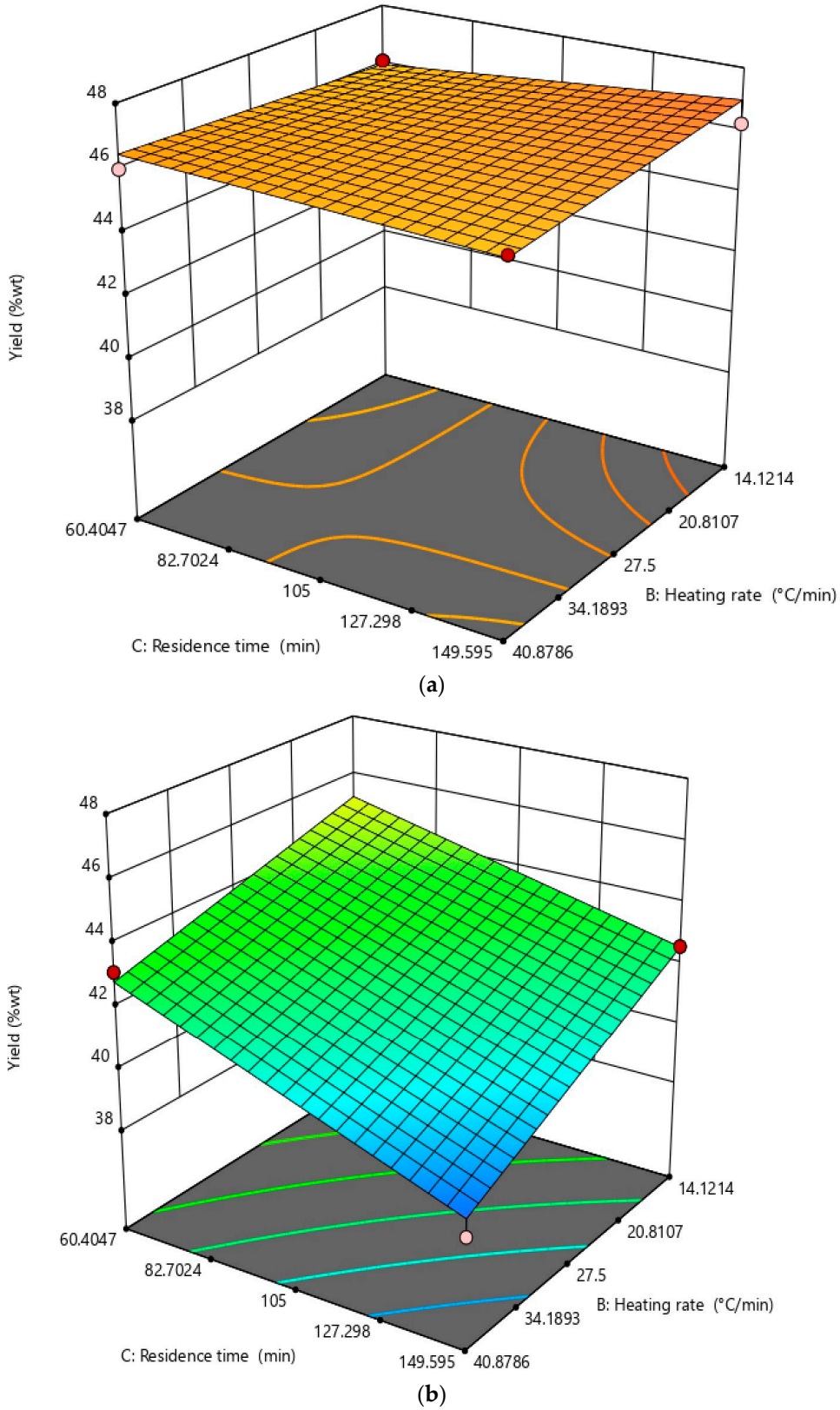

Figure 5. Response of biochar yield (wt%) to residence time and heating rate at 490.5 °C (**a**) and 609.5 °C (**b**). Red and pink dots indicate the domain limits.

In the studied temperature range, higher temperatures favored a greater decomposition and subsequent higher volatilization of the sewage sludge. As a result, the residual

solid matter decreased. Many authors reported that the increase in pyrolysis temperature resulted in a significant decrease in biochar yield [26,45]: higher temperatures correspond to a greater primary decomposition of the initial feedstock or to secondary reactions of the solid residue. As already seen, run 4, which is the run carried out at the lowest temperature, obtained the highest biochar yield. Figure 5a shows how at 490.5 °C, biochar yield is weakly dependent on heating rate and residence time: in particular, biochar yield slightly decreased with heating rate and slightly increased with residence time. The shape of the 3D curve obtained at 609.5 °C (Figure 5b) is completely different from that at 490.5 °C: temperature heavily affected how heating rate and residence time influenced the variable studied since in Equations (5) and (6) the two-factor interaction terms involving temperature, AB and AC, appear. At 609.5 °C, a fast heating rate and long residence time cause a more complete degradation of the sewage sludge solid matrix towards the liquid bio-oil and gas fractions [23,46].

Therefore, to increase the biochar yield, it may be interesting to study a lower temperature range, probably to the detriment of the CO_2 adsorption capacity of produced biochar. The CO_2 adsorption capacity could be improved by physical or chemical activation of biochar in a subsequent step [20]. The observation that yields and CO_2 adsorption capacity do not exhibit the same trend, with respect to the studied parameters implies that CO_2 adsorption capacity is not solely contingent upon the quantity of biochar produced (since we are considering the ash content of biochar). Rather, it is influenced by the distinct morphology and chemical physical structure of biochar generated by different runs.

In light of the results regarding both biochar yield and CO_2 adsorption capacity, the DoE software provided the optimal parameters to produce biochar from sewage sludge by pyrolysis, prioritizing the CO_2 adsorption capacity. These parameters correspond to those set for run 2.

3.3. Biochar Produced by a Semi-Batch Bench Scale Reactor

The results obtained in terms of yield and CO_2 adsorption capacity for biochar produced by the "best experiment" and "worst experiment" (chosen among the run with a heating rate of 14.12 °C/min, run 2 and run 14 of the DoE CCD, respectively) in a semi-batch bench scale reactor are shown in Table 7. The CO_2 adsorption was preceded by a purge phase (from 25 °C to the biochar synthesis temperature minus 10 °C) where the samples lost weight (6–7 wt%) prior to reaching a constant value and starting the CO_2 adsorption. This weight loss was due to the release of gasses/vapors (mainly, humidity and the CO_2 of the air) adsorbed by the carbonaceous structure of the sample during its storage. This purge was not carried out during the TGA runs of DoE CCD, since pyrolysis was immediately followed by CO_2 adsorption tests without any contact between biochar and ambient air.

Table 7. Biochar yield and CO_2 adsorption capacity obtained in a semi-batch bench scale reactor adopting the "best" and "worst" experimental parameters resulting from DoE.

Test	Temperature (°C)	Heating Rate (°C/min)	Residence Time (min)	Experimental Yield (wt%)	Experimental Adsorption Capacity (mol CO_2 ads/kg)	Theoretical Yield (wt%)	Theoretical Adsorption Capacity (mol CO_2 ads/kg)
"Best" biochar	491	20	150	43.9	0.735	46.8	0.476
"Worst" biochar	610	20	60	42.7	0.625	44.7	0.427

As can be observed, the predictions of DoE were correct: the "best" operating parameters really led to a higher biochar yield and this biochar was characterized by a higher CO_2 adsorption capacity in comparison to those obtained with the "worst" operating parameters. As expected, in the studied ranges, lower temperature and higher residence time (the heating rate could not be modified in this pyrolysis system) both enhanced the quality of the produced biochar, while their effect was in contrast in terms of yield. On

the other hand, experimental and theoretical values (those calculated by Equations (4) and (6) of DoE for the set parameters) were different: the experimental yield was lower than the theoretical one, while the experimental adsorption capacity was significantly higher. The average relative errors between the experimental and calculated values were 6 and 33% for biochar yield and CO_2 adsorption capacity, respectively. Especially in the case of CO_2 adsorption capacity, these errors are higher in comparison to those determined for TGA experiments (0.2% and 3%, respectively). These discrepancies were caused by the different experimental set-ups. Indeed, the Lenton system was characterized by a worse control of process parameters (i.e., temperature, heating rate, time, N_2 flow rate) compared to the TGA, and the nitrogen produced by the generator was not as pure as that used for TGA. Furthermore, the two pieces of equipment had different lengths and geometries of the reaction chamber with different fluid dynamics, although the velocity of the gas in the reactor was kept constant, and different contact surfaces between the sample and the gas carrier. It is well known that even the flow of the inert gas is an important parameter in the pyrolysis process, influencing the yield and the quality of the products [47]. Lastly, the sample had the following different characteristics: quantity (from milligram to gram for TGA and Lenton, respectively) and granulometry (from uniform < 0.5 mm to non-uniform < 20 mm for TGA and Lenton, respectively). All these differences caused an improvement in CO_2 adsorption capacity with a slightly lower biochar yield. This result showed how, although the parameters related to temperature and time are extremely important in a pyrolysis process, different reaction systems lead to different results regarding CO_2 adsorption capacity and biochar yield in absolute terms, despite the general trend being respected. CO_2 adsorption capacity seems to be more sensitive to these modifications in comparison to the biochar yield.

Table 8 shows the specific surface area, volume and average pore size of dried sewage sludge, "best" and "worst" biochar, determined by BET/BJH analysis. Figures S10 and S11 depict their adsorption/desorption and pore distribution curves, respectively. The analyzed samples exhibit a type IV isotherm with a hysteresis loop (Figure S10) attributed to capillary condensation within mesopores (20 < d < 500 Å) at the relative pressure range of 0.45–0.99 p/p^0. The lower adsorption at $p/p^0 < 0.4$ and the higher adsorption at $p/p^0 > 0.9$ suggest that the biochars had a number of micropores (d < 20 Å) and macropores (d > 500 Å), respectively. According to the IUPAC classification, the hysteresis loops are categorized as type H3, with a minor presence of type H4. This indicates that slit-shaped or wedge-shaped pores are predominant in the samples [48].

Table 8. Surface area and pore characteristics of dried sewage sludge, "best" and "worst" biochar.

Sample	Surface Area (m^2/g)	Micropore Area (m^2/g)	Pore Volume (cm^3/g)	Micropore Volume (cm^3/g)	Pore Average Diameter (Å)
Sewage Sludge	0.46	0.23	0.004	0.000081	205.37
"Best" biochar	123.85	97.03	0.063	0.038	88.69
"Worst" biochar	102.91	86.85	0.051	0.034	104.08

While dried sewage sludge had a negligible surface area of 0.46 m^2/g, the "best" and "worst" biochar were characterized by a surface area of 123.85 and 102.91 m^2/g, respectively. Pyrolysis of different biomass feedstocks produced biochars with a wide range of surface area (0.1–570 m^2/g) [49].

In the adsorption isotherm of the dried sewage sludge, the quantity of N_2 adsorbed at low relative pressures increases slowly compared to that of biochars, indicating poorly developed micropores. Indeed, according to the t-plot method, the micropore area in the dried sewage sludge accounts for only 50% of the total specific surface area, compared to almost 78% and 84% for the "best" and "worst" biochar, respectively (Table 8).

As shown in Figure S11A, the pore size distribution of the sewage sludge sample is narrower and multimodal, with predominant pores in the diameter range of 136.1–98.5 Å. The differential pore volume (Figure S11B) shows a shift of the peak corresponding to small

pores from 63.2 to 52.7 Å to 40.6–36.2 Å in the biochar samples. Additionally, the volume of mesopores in the samples increases notably compared to the sewage sludge, with a greater amount observed in the "best" biochar. Moreover, a shift in the micropore region is evident in Figure S11B, indicating a pronounced increase in the presence of smaller pores in the "best" biochar sample.

In general, the BET-specific surface area, pore size and pore volume all have a positive impact on the CO_2 adsorption capacity of biochar. High temperature or subsequent physical or chemical activation led to biochar with a higher surface area.

This is due to the release of volatile organic compounds from the raw material structure, which creates porous networks and increases the total specific surface area. As a result, more active sites become available for interactions between CO_2 and biochar. However, studies have demonstrated that CO_2 adsorption capacity correlates more strongly with micropore surface area than with BET surface area [50]. Additionally, the volume and surface area of micropores in biochar typically increase with higher pyrolysis temperatures. Nevertheless, temperatures above 500 °C may lead to an opposite trend, as neighboring pores can coalesce, potentially enlarging the pores (creating mesopores and macropores) and reducing their overall volume [22].

According to Zhang et al. [51], the role of biochar pores in capturing CO_2 can be summarized as follows: macropores facilitate diffusion CO_2 diffusion throughout the bulk of biochar, while mesopores serve as transport channels that allow CO_2 to move unrestrictedly and reach the micropores. These latter serve as the main sites for CO_2 adsorption and retention, allowing CO_2 to be fixed within the biochar material.

The adsorption properties of biochar are closely related to its carbon content, which may vary based on the conditions under which the feedstock undergoes pyrolysis. However, drastic thermal/physical/chemical conditions could cause high volatilization and produce a solid residue mainly composed of ash. Pelagalli et al. [20], in their review on pyrolysis of municipal sewage sludge, reported biochar obtained by several studies with a narrower range of surface area (0.1–70 m^2/g) and with a high ash content (52–92 wt%).

Table 9 reports some other features of the two biochars. As far as the organic fraction is concerned, carbon was the main element, and the "best biochar" still had 21 wt% of volatile matter, while the fixed carbon is equal to about 13 wt%. The weight loss at 105 °C corresponds to the moisture content with a value similar to that obtained during the purge of biochar before the CO_2 adsorption test. "Best biochar" was mainly composed of ash that, being the inorganic fraction, was unaltered by pyrolysis and accumulated into the solid phase. The "worst biochar" had similar characteristics with a slightly lower moisture content and higher ash content. Because of the high ash content, LHV was around 6–7 MJ/kg. The high ash content also limited the CO_2 adsorption capacity. Indeed, the CO_2 adsorption capacity of ashes obtained after combustion at 550 °C for 1 h of a "best biochar" sample resulted as null under these experimental conditions. Therefore, calculating the CO_2 adsorption capacity of the biochar net of the ash content, it was found to significantly increase from 0.735 to 1.87 mol CO_2/kg, in the case of "best biochar". In the future, it might be interesting to study how the CO_2 adsorption capacity may vary for different pyrolysis parameters net of biochar ash content. Even if the organic and the inorganic components of biochar cannot be separated in real terms, it would be interesting to correlate the CO_2 adsorption capacity only to the morphology and chemical physical characteristics of its carbonaceous structure. This approach could even improve the reliability of the CO_2 adsorption capacity model obtained by DoE.

Table 9. Proximate, ultimate and LHV analysis of "best" and "worst" biochar.

Sample	Moisture (wt%)	Volatile Matter (wt%)	Fixed Carbon (wt%)	Ashes (wt%)	C (wt%)	H (wt%)	N (wt%)	S (wt%)	O * (wt%)	LHV (MJ/kg)
"Best" biochar	5.6 ± 0.1	21.1 ± 0.4	12.7 ± 0.3	60.6 ± 0.1	23.1 ± 0.4	0.40 ± 0.04	3.2 ± 0.1	0.40 ± 0.01	12.3	6.78 ± 0.09
"Worst" biochar	4.8 ± 0.2	17.5 ± 0.5	14.1 ± 0.8	63.7 ± 0.9	22.8 ± 1.7	0.2 ± 0.1	2.5 ± 0.2	0.5 ± 0.1	10.4	5.95 ± 0.07

* Oxygen is calculated by difference.

3.4. Theoretical Energy Balance

The energy consumption associated with the pyrolysis process of digested and centrifuged sewage sludge can be divided into two phases: drying and pyrolysis, the latter divided into heating and thermal degradation. In this theoretical energy balance the energy is simply supplied through the complete combustion of the dried sewage sludge (i.e., by its LHV), without considering the heat recovered from the hot fumes.

For the drying phase, the energy balance is

$$M_{dss} \cdot LHV = c_{pSS} \cdot M_{TQ} \cdot \Delta T + M_W \cdot \lambda \quad (7)$$

where M_{dSS} is the mass (kg) of dried sewage sludge to burn in order to dry 1 t of centrifuged sewage sludge;

LHV is the low heating value (MJ/kg) of dried sewage sludge;

c_{pSS} is the specific heat (J/(kg °C)) of sewage sludge;

M_{TQ} is the mass (kg) of centrifuged sewage sludge;

ΔT is the temperature difference (°C) between drying temperature (105 °C) and ambient temperature (25 °C);

M_W is the mass (kg) of water in the centrifuged sewage sludge;

λ is the water latent heat of evaporation (2257 kJ/kg).

The c_{pSS} was calculated with the following equations [52]:

$$c_{pSS} = c_{pW} \frac{X}{1+X} + c_{pDM} \frac{1}{1+X} \quad (8)$$

$$c_{pDM} = 1434 + 3.29 \cdot T \quad (9)$$

where c_{pW} is the specific heat (4187 J/(kg °C)) of water;

c_{pDM} is the specific heat (J/(kg °C)) of dried sewage sludge;

X is the weight fraction of water in dried sewage sludge;

T is the temperature of dried sewage sludge.

If M_{TQ} is 1000 kg with a water content of 75.6 wt%, M_W is 756 kg and X is 3.1. The c_{pDM} was calculated at 25 °C, assuming that the variations of c_{pDM} are insignificant for the energy balance in the considered temperature range. Consequently, it results in c_{pDM} =1516.25 J/(kg °C) and c_{pSS} =3535.34 J/(kg °C). Then, from Equation (7) we obtained

$$M_{dss} = \frac{c_{pSS} \cdot M_{TQ} \cdot \Delta T + M_W \cdot \lambda}{LHV} = 144.7 \text{ kg} \quad (10)$$

Therefore, the energy needs for the drying process of 1 ton of centrifuged sewage sludge with a moisture content of 75.6 wt% require burning more than half (59 wt%) of the dry matter present in the sewage sludge.

The second phase concerns the heating of the dried sewage sludge up to the degradation temperature and the heat needed for thermal degradation (from the endothermic peaks of the DSC curve). Then, the overall energy needed for the thermal pyrolysis of the dried sewage sludge was calculated according to Equation (11):

$$M_{dss} \cdot LHV = c_{ps} \cdot (M_{dss})_p \cdot \Delta T + Q_D \cdot (M_{dss})_p \quad (11)$$

where M_{dss} is the mass (kg) of dried sewage sludge to burn in order to pyrolyze 1 t of dried sewage sludge;

$(M_{dss})_p$ is the mass (kg) of dried sewage sludge to pyrolyze;

LHV is the low heating value (MJ/kg) of dried sewage sludge;

c_{ps} is the specific heat of the sample (1008 J/(kg °C), experimentally derived from the DSC curve;

ΔT is the temperature difference (°C) between an intermediate degradation temperature (319 °C) and the drying temperature (105 °C);

Q_D is the degradation heat (MJ/kg) associated with the three endothermic peaks of the DSC curve connected to the pyrolysis process (109,000, 14,000 and 6000 J/kg).

Writing Equation (11) as carried out for Equation (10), we obtained

$$M_{dss} = \frac{(M_{dss})_p(c_{pDM} \cdot \Delta T + Q_D)}{LHV} = 25.1 \text{ kg} \quad (12)$$

The energy needs for the pyrolysis process of 1 ton of dried sewage sludge require burning about 10 wt% of the dry matter present in the sewage sludge. More commonly, the required energy can be supplied by the combustion of a fraction of the pyrolysis products and exploiting the relative heat recovery.

Comparing the results of Equations (10) and (12), the extremely high energy needs of the drying phase are evident. Innovative dewatering processes for sewage sludge such as filter press technology [53], dewatering electrodehydration [54], geotexil tube [55] together with innovative drying processes such as solar drying [56] could lower the energy needs due to the water content of the sewage sludge entering the pyrolysis plant and increase its energy efficiency.

4. Conclusions

This paper reports and analyzes the results of the optimization by DoE software of three parameters (temperature, heating rate and residence time) for the pyrolysis process aimed at the production of biochar from municipal sewage sludge. Biochar production was evaluated in terms of yield and CO_2 adsorption capacity.

A two-factor interaction model provided satisfactory results for both yield and CO_2 adsorption capacity. The yield model proved to be more accurate, while the CO_2 adsorption capacity model could have been affected by the yield results (i.e., the presence of inert ash in the biochar). Pyrolysis temperature was the most critical factor affecting the yield of biochar produced, while heating rate and residence time, expressed as a two-factor interaction term, had the highest "weight" for its CO_2 adsorption capacity. The yield decreased with increasing temperatures, heating degrees and residence time, which favored the decomposition of volatile matter. Instead, the CO_2 adsorption capacity first increased and then decreased with increasing temperature. Higher CO_2 adsorption capacity was also obtained for slow heating rates at long residence times and for short residence times at high heating rates. Furthermore, the results showed that yield and CO_2 adsorption capacity are not directly correlated: considering the presence of inert ash, more biochar does not necessarily correspond to more CO_2 adsorbed. Temperature, heating rate and residence time influence the chemical and physical features of the produced biochar.

The transition to a larger-scale reactor confirmed the trend predicted by DoE, but the values of yield and CO_2 adsorption capacity were quite different from those forecasted by the model.

In conclusion, this study highlighted how the selection of proper operating conditions is a crucial step in the design of an industrial process for the production of biochar from sewage sludge since it can have a strong impact on its economic and technological sustainability. The percentage differences between the minimum and maximum values obtained by the different tests can reach 20 and 39% for yield and CO_2 adsorption capacity, respectively.

The theoretical energy balance showed that the pyrolysis of centrifuged sewage sludge is energy-intensive, with the drying phase being the most costly stage. New solutions

are necessary to reduce the water content of the feedstock and optimize the utilization of energy from the pyrolysis products. Future research should focus on developing more efficient drying techniques and exploring ways to integrate heat recovery systems into the process.

Supplementary Materials: The following supporting information can be downloaded at https://www.mdpi.com/article/10.3390/environments11100210/s1. Table S1: TGA thermal program for proximate analysis; Figure S1: Dried sewage sludge out from the oven; Figure S2: Actual vs. predicted plot of CO_2 adsorption capacity ($molCO_2/kg$); Figure S3: Normal plot of residuals of CO_2 adsorption capacity; Figure S4: Residuals vs. predicted values of CO_2 adsorption capacity ($molCO_2/kg$); Figure S5: Residuals vs. run number of CO_2 adsorption capacity; Figure S6: Actual vs. predicted plot of biochar yield (wt%); Figure S7: Normal plot of residuals of biochar yield; Figure S8: Residuals vs. predicted values of biochar yield (wt%); Figure S9: Residuals vs. run number of biochar yield; Figure S10: N_2 adsorption–desorption isotherms of dried sewage sludge. "best" and "worst" biochar; Figure S11: Pore volume distribution and incremental pore area of (A) dried sewage sludge. (B) "best" and "worst" biochar.

Author Contributions: Conceptualization, R.T. and M.S.; methodology, R.T. and M.L.; validation, L.C.; formal analysis, G.C.; investigation, G.C., M.P.B. and L.C.; writing—original draft preparation, R.T., M.P.B. and M.L.; writing—review and editing, R.T. and M.S.; supervision, M.S.; project administration, D.M.; funding acquisition, D.M. All authors have read and agreed to the published version of the manuscript.

Funding: This research was funded by the Project "Energy efficiency of industrial products and processes"–Research program: "Piano Triennale della Ricerca del Sistema Elettrico Nazionale 2022–2024" funded by the Italian Ministry of Economic Development.

Data Availability Statement: Data are contained within the article or Supplementary Materials.

Conflicts of Interest: The authors declare no conflicts of interest.

References

1. Bagheri, M.; Bauer, T.; Burgman, L.E.; Wetterlund, E. Fifty years of sewage sludge management research: Mapping researchers' motivations and concerns. *J. Environ. Manag.* **2023**, *325*, 116412. [CrossRef] [PubMed]
2. European Commission. A New Circular Economy Action Plan. Available online: https://www.un.org/sustainabledevelopment/sustainable-consumption-production/ (accessed on 16 September 2024).
3. European Commission. *Bioeconomy: The European Way to Use Our Natural Resources: Action Plan 2018*; European Commission, Directorate-General for Research and Innovation: Brussels, Belgium, 2018. [CrossRef]
4. European Parliament and the Council. Regulation (EU) 2019/1009 of 5 June 2019 Laying Down Rules on the Making Available on the Market of EU Fertilising Products and Amending Regulations (EC) No 1069/2009 and (EC) No 1107/2009 and Repealing Regulation (EC) No 2003/2003. Available online: https://eur-lex.europa.eu/eli/reg/2019/1009/oj (accessed on 16 September 2024).
5. European Commission. Farm to Fork Strategy for a Fair, Healthy and Environmentally-Friendly Food System. Available online: https://food.ec.europa.eu/horizontal-topics/farm-fork-strategy_en (accessed on 16 September 2024).
6. European Commission. Biodiversity Strategy for 2030 Bringing Nature Back into Our Lives. Available online: https://ec.europa.eu/research/environment/index.cfm?pg=nbs (accessed on 16 September 2024).
7. European Commission. EU Soil Strategy for 2030 Reaping the Benefits of Healthy Soils for People, Food, Nature and Climate. Available online: https://www.eea.europa.eu/data-and-maps/dashboards/land-take-statistics#tab-based-on-data (accessed on 16 September 2024).
8. European Commission. *Strategic Plan 2020–2024 DG Climate Action*. European Commission 2020. Available online: https://commission.europa.eu/publications/strategic-plan-2020-2024-climate-action_en (accessed on 16 September 2024).
9. Eurostat. Sewage Sludge Production and Disposal from Urban Wastewater. Available online: https://ec.europa.eu/eurostat/databrowser/view/ten00030/default/table?lang=en (accessed on 12 June 2024).
10. ISPRA. *Rapporto Rifiuti Speciali*; ISPRA: Rome, Italy, 2021; ISBN 978-88-448-1052-8.
11. European Commission. The Commission Decides to Refer ITALY to the Court of Justice of the European Union for Failure to Fully Comply with the Urban Wastewater Treatment Directive. Available online: https://ec.europa.eu/commission/presscorner/detail/en/ip_24_1234 (accessed on 18 June 2024).
12. Volpi, M.P.C.; Silva, J.C.G.; Hornung, A.; Ouadi, M. Review of the Current State of Pyrolysis and Biochar Utilization in Europe: A Scientific Perspective. *Clean Technol.* **2024**, *6*, 152–175. [CrossRef]
13. Nakao, S.; Yogo, K.; Goto, K.; Kai, T.; Yamada, H. *Advanced CO_2 Capture Technologies*; Springer International Publishing: Cham, Switzerland, 2019. [CrossRef]

14. Karimi, M.; Shirzad, M.; Silva, J.A.C.; Rodrigues, A.E. Biomass/Biochar carbon materials for CO_2 capture and sequestration by cyclic adsorption processes: A review and prospects for future directions. *J. CO_2 Util.* **2022**, *57*, 101890. [CrossRef]
15. Ozkan, M.; Akhavi, A.A.; Coley, W.C.; Shang, R.; Ma, Y. Progress in carbon dioxide capture materials for deep decarbonization. *Chem* **2022**, *8*, 141–173. [CrossRef]
16. Sharma, A.K.; Ghodke, P.K.; Chen, W.H. Progress in green adsorbent technologies from sewage sludge for wastewater remediation and carbon capture: A sustainable approach towards clean environment. *Curr. Opin. Green Sustain. Chem.* **2024**, *46*, 100883. [CrossRef]
17. Leng, L.; Xiong, Q.; Yang, L.; Li, H.; Zhou, Y.; Zhang, W.; Jiang, S.; Li, H.; Huang, H. An overview on engineering the surface area and porosity of biochar. *Sci. Total. Environ.* **2021**, *763*, 144204. [CrossRef]
18. Dissanayake, P.D.; Choi, S.W.; Igalavithana, A.D.; Yang, X.; Tsang, D.C.; Wang, C.-H.; Kua, H.W.; Lee, K.B.; Ok, Y.S. Sustainable gasification biochar as a high efficiency adsorbent for CO_2 capture: A facile method to designer biochar fabrication. *Renew. Sustain. Energy Rev.* **2020**, *124*, 109785. [CrossRef]
19. Yadav, K.; Jagadevan, S. Influence of Process Parameters on Synthesis of Biochar by Pyrolysis of Biomass: An Alternative Source of Energy. In *Recent Advances in Pyrolysis*; IntechOpen: London, UK, 2020. [CrossRef]
20. Pelagalli, V.; Langone, M.; Matassa, S.; Race, M.; Tuffi, R.; Papirio, S.; Lens, P.N.L.; Lazzazzara, M.; Frugis, A.; Pettag, L.; et al. Pyrolysis of municipal sewage sludge: Challenges, opportunities and new valorization routes for biochar, bio-oil, and pyrolysis gas. *Environ. Sci. Water Res. Technol.* **2024**. [CrossRef]
21. Demirbas, A. Effects of temperature and particle size on bio-char yield from pyrolysis of agricultural residues. *J. Anal. Appl. Pyrolysis* **2004**, *72*, 243–248. [CrossRef]
22. Angin, D. Effect of pyrolysis temperature and heating rate on biochar obtained from pyrolysis of safflower seed press cake. *Bioresour. Technol.* **2013**, *128*, 593–597. [CrossRef]
23. Verrecchia, G.; Cafiero, L.; de Caprariis, B.; Dell'Era, A.; Pettiti, I.; Tuffi, R.; Scarsella, M. Study of the parameters of zeolites synthesis from coal fly ash in order to optimize their CO_2 adsorption. *Fuel* **2020**, *276*, 118041. [CrossRef]
24. Kaur, L.; Singh, J.; Ashok, A.; Kumar, V. Design expert based optimization of the pyrolysis process for the production of cattle dung bio-oil and properties characterization. *Sci. Rep.* **2024**, *14*, 9421. [CrossRef]
25. Cha, J.S.; Park, S.H.; Jung, S.-C.; Ryu, C.; Jeon, J.-K.; Shin, M.-C.; Park, Y.-K. Production and utilization of biochar: A review. *J. Ind. Eng. Chem.* **2016**, *40*, 1–15. [CrossRef]
26. Agrafioti, E.; Bouras, G.; Kalderis, D.; Diamadopoulos, E. Biochar production by sewage sludge pyrolysis. *J. Anal. Appl. Pyrolysis* **2013**, *101*, 72–78. [CrossRef]
27. Inguanzo, M.; Domínguez, A.; Menéndez, J.A.; Blanco, C.G.; Pis, J.J. On the Pyrolysis of Sewage Sludge: The Influence of Pyrolysis Conditions on Solid, Liquid and Gas Fractions. *J. Anal. Appl. Pyrolysis* **2002**, *63*, 209–222. [CrossRef]
28. Hu, M.; Hu, H.; Ye, Z.; Tan, S.; Yin, K.; Chen, Z.; Guo, D.; Rong, H.; Wang, J.; Pan, Z.; et al. A review on turning sewage sludge to value-added energy and materials via thermochemical conversion towards carbon neutrality. *J. Clean. Prod.* **2022**, *379*, 134657. [CrossRef]
29. Cafiero, L.; Fabbri, D.; Trinca, E.; Tuffi, R.; Ciprioti, S.V. Thermal and spectroscopic (TG/DSC-FTIR) characterization of mixed plastics for materials and energy recovery under pyrolytic conditions. *J. Therm. Anal. Calorim.* **2015**, *121*, 1111–1119. [CrossRef]
30. Huang, H.J.; Yuan, X.Z. The migration and transformation behaviors of heavy metals during the hydrothermal treatment of sewage sludge. *Bioresour. Technol.* **2016**, *200*, 991–998. [CrossRef]
31. Zhao, C.; Hong, C.; Hu, J.; Xing, Y.; Ling, W.; Zhang, B.; Wang, Y.; Feng, L. Upgrading technologies and catalytic mechanisms for heteroatomic compounds from bio-oil—A review. *Fuel* **2023**, *333*, 126388. [CrossRef]
32. Esposito, L.; Cafiero, L.; De Angelis, D.; Tuffi, R.; Ciprioti, S.V. Valorization of the plastic residue from a WEEE treatment plant by pyrolysis. *Waste Manag.* **2020**, *112*, 1–10. [CrossRef]
33. Gao, N.; Li, J.; Qi, B.; Li, A.; Duan, Y.; Wang, Z. Thermal analysis and products distribution of dried sewage sludge pyrolysis. *J. Anal. Appl. Pyrolysis* **2014**, *105*, 43–48. [CrossRef]
34. Hu, M.; Ye, Z.; Zhang, H.; Chen, B.; Pan, Z.; Wang, J. Thermochemical conversion of sewage sludge for energy and resource recovery: Technical challenges and prospects. *Environ. Pollut. Bioavailab.* **2021**, *33*, 145–163. [CrossRef]
35. Kan, T.; Grierson, S.; De Nys, R.; Strezov, V. Comparative assessment of the thermochemical conversion of freshwater and marine micro- and macroalgae. *Energy Fuels* **2014**, *28*, 104–114. [CrossRef]
36. Magdziarz, A.; Werle, S. Analysis of the combustion and pyrolysis of dried sewage sludge by TGA and MS. *Waste Manag.* **2014**, *34*, 174–179. [CrossRef] [PubMed]
37. Liu, C.; Wu, Y.; Lan, G.; Ji, X.; Xia, Y.; Fu, C.; Shen, J.; Gui, J.; Liu, Y.; Qu, Y.; et al. CO_2 capture performance of biochar prepared from sewage sludge after conditioning with different dewatering agents. *J. Environ. Chem. Eng.* **2022**, *10*, 108318. [CrossRef]
38. Xu, X.; Kan, Y.; Zhao, L.; Cao, X. Chemical transformation of CO_2 during its capture by waste biomass derived biochars. *Environ. Pollut.* **2016**, *213*, 533–540. [CrossRef]
39. Samanta, A.; Zhao, A.; Shimizu, G.K.H.; Sarkar, P.; Gupta, R. Post-Combustion CO_2 Capture Using Solid Sorbents: A Review. *Ind. Eng. Chem. Res.* **2012**, *51*, 1438–1463. [CrossRef]
40. Fonts, I.; Azuara, M.; Gea, G.; Murillo, M.B. Study of the pyrolysis liquids obtained from different sewage sludge. *J. Anal. Appl. Pyrolysis* **2009**, *85*, 184–191. [CrossRef]

41. Hossain, M.K.; Strezov, V.; Nelson, P.F. Thermal characterisation of the products of wastewater sludge pyrolysis. *J. Anal. Appl. Pyrolysis* **2009**, *85*, 442–446. [CrossRef]
42. Lu, G.Q.; Low, J.C.F.; Liu, C.Y.; Lua, A.C. Surface area development of sewage sludge during pyrolysis. *Fuel* **1995**, *74*, 344–348. [CrossRef]
43. Anuar Sharuddin, S.D.; Abnisa, F.; Wan Daud, W.M.A.; Aroua, M.K. A review on pyrolysis of plastic wastes. *Energy Convers. Manag.* **2016**, *115*, 308–326. [CrossRef]
44. Ghodke, P.K.; Sharma, A.K.; Pandey, J.K.; Chen, W.H.; Patel, A.; Ashokkumar, V. Pyrolysis of sewage sludge for sustainable biofuels and value-added biochar production. *J. Environ. Manag.* **2021**, *298*, 113450. [CrossRef]
45. Hossain, M.K.; Vladimir, V.S.; Chan, K.Y.; Ziolkowski, A.; Nelson, P.F. Influence of pyrolysis temperature on production and nutrient properties of wastewater sludge biochar. *J. Environ. Manag.* **2011**, *92*, 223–228. [CrossRef] [PubMed]
46. Gao, N.; Quan, C.; Liu, B.; Li, Z.; Wu, C.; Li, A. Continuous Pyrolysis of Sewage Sludge in a Screw-Feeding Reactor: Products Characterization and Ecological Risk Assessment of Heavy Metals. *Energy Fuels* **2017**, *31*, 5063–5072. [CrossRef]
47. Encinar, J.M.; González, J.F. Pyrolysis of synthetic polymers and plastic wastes. Kinetic study. *Fuel Process. Technol.* **2008**, *89*, 678–686. [CrossRef]
48. Sing, K.S.W.; Everett, D.H.; Haul, R.A.W.; Moscou, L.; Pierotti, R.A.; Rouquerol, J.; Siemieniewska, T. Reporting physisorption data for gas/solid systems with special reference to the determination of surface area and porosity (Recommendations 1984). *Pure Appl. Chem.* **1985**, *57*, 603. [CrossRef]
49. Mamaghani, Z.G.; Hawboldt, K.A.; MacQuarrie, S. Adsorption of CO_2 using biochar—Review of the impact of gas mixtures and water on adsorption. *J. Environ. Chem. Eng.* **2023**, *11*, 109643. [CrossRef]
50. Zhang, Z.; Zhou, J.; Xing, W.; Xue, Q.; Yan, Z.; Zhuo, S.; Qiao, S.Z. Critical role of small micropores in high CO_2 uptake. *Phys. Chem. Chem. Phys.* **2013**, *15*, 2523. [CrossRef] [PubMed]
51. Zhang, C.; Ji, Y.; Li, C.; Zhang, Y.; Sun, S.; Xu, Y.; Jiang, L.; Wu, C. The Application of Biochar for CO_2 Capture: Influence of Biochar Preparation and CO_2 Capture Reactors. *Ind. Eng. Chem. Res.* **2023**, *62*, 17168–17181. [CrossRef]
52. Arlabosse, P.; Chavez, S.; Prevot, C. Drying of Municipal Sewage Sludge: From a Laboratory Scale Batch Indirect Dryer to the Paddle Dryer. *Braz. J. Chem. Eng.* **2005**, *22*, 227–232. [CrossRef]
53. Hou, J.; Hong, C.; Ling, W.; Hu, J.; Feng, W.; Xing, Y.; Wang, Y.; Zhao, C.; Feng, L. Research progress in improving sludge dewaterability: Sludge characteristics, chemical conditioning and influencing factors. *J. Environ. Manag.* **2024**, *351*, 119863. [CrossRef] [PubMed]
54. Lee, N.Y.; You, M.Y.; Lee, J.; Kim, S.; Song, P.K. Performance of Insoluble IrO_2 Anode for Sewage Sludge Cake Electrodehydration Application with Respect to Operation Conditions. *Coatings* **2022**, *12*, 724. [CrossRef]
55. Ardila, M.A.A.; de Souza, S.T.; da Silva, J.L.; Valentin, C.A.; Dantas, A.D.B. Geotextile tube dewatering performance assessment: An experimental study of sludge dewatering generated at a water treatment plant. *Sustainability* **2020**, *12*, 8129. [CrossRef]
56. Jangde, P.K.; Singh, A.; Arjunan, T.V. Efficient solar drying techniques: A review. *Environ. Sci. Pollut. Res.* **2022**, *29*, 50970–50983. [CrossRef] [PubMed]